PROCEEDINGS OF SCIENCE

Detailed KM3NeT optical module simulation with Geant4 and supernova neutrino detection study

Marta Colomer
APC, Univ Paris Diderot, CNRS/IN2P3, CEA/IRFU, Observatoire de Paris, Soborne Paris Cité, France
E-mail: marta.colomer-molla@u-psud.fr

Damien Dornic* **and Vladimir Kulikovskiy**
Aix Marseille Univ, CNRS/IN2P3, CPPM, Marseille, France
E-mail: kulikovskiy@cppm.in2p3.fr

on behalf of the KM3NeT collaboration

A detailed Geant4 simulation originally created for ANTARES optical modules (OM) has been improved to include the KM3NeT directional OM simulation. Optical modules are reproduced following technical drawings. Standard low-energy physics processes are combined with response of bialkali photocathodes. The simulation setup is easily reconfigurable for various OMs and environments (air, water). In particular, this simulation software is used to study the feasibility of supernova neutrino detection with KM3NeT.

Although KM3NeT detectors are mainly designed for high-energy neutrino detection, the MeV neutrino signal from a supernova can be identified as a simultaneous increase of the counting rate of the optical modules in the detector. The light is mainly emitted by MeV positrons produced by neutrinos interacting with free protons in water, inverse beta decay. The noise from the optical background due to K40 decays in sea water and bioluminescence can be significantly reduced by using nanosecond coincidences between the nearby placed PMTs. This technique has been tested with the ANTARES storeys consisting of three 10-inch PMTs and is optimized for the KM3NeT telescope where the directional OMs containing 31 3-inch PMT provide very promising expectations.

35th International Cosmic Ray Conference — ICRC2017
10–20 July, 2017
Bexco, Busan, Korea

*Speaker.

PoS(ICRC2017)983

1. Introduction

ANTARES and KM3NeT are neutrino telescopes with three-dimensional photomultiplier (PMT) arrays in the deep sea water well shielded from atmospheric muons. Such telescopes can be used to study different evolution stages of the SuperNova (SN) explosions: prompt supernova emission (MeV), transient high energy neutrino emission (GeV–TeV) from GRB-SN and Super Novae Remnants (SNR) steady neutrino emission (GeV–TeV). Neutrino event reconstruction is efficient for GeV energies and above for such detectors and defined by the PMT density. The GRB-SN and SNR detection strategies involve neutrino event reconstruction and their discrimination from the atmospheric background [1, 2]. The ANTARES participation in multi-messenger programs exploits the high connection between neutrinos and other cosmic messengers: electromagnetic signals, from X-rays to high-energy gamma-rays, charged cosmic rays, gravitational waves [3, 4]. Multi-messenger programs are looking forward the KM3NeT participation[1]. The description of these high-energy neutrino analyses are presented by both collaborations in this conference.

Prompt SN emission (MeV neutrinos) should produce an increase of PMT rates in the detector. Event reconstruction is not possible but high sensitivity in time domain is expected for such observations. Prompt emission models and search optimization for KM3NeT are discussed here.

2. Detector technologies

The ANTARES detector is the first undersea neutrino telescope. It is installed at 2475 m depth; its effective mass is about 10 Mt and its detection energy threshold is about tens GeV [5]. KM3NeT is a distributed research infrastructure that will host at Phase 2 a high energy (TeV-PeV) neutrino telescope (ARCA), offshore of Capo Passero, and an atmospheric neutrino detector (ORCA), offshore of Toulon in France (close to the ANTARES site), for the determination of the neutrino mass hierarchy [1]. ARCA has two detector blocks instrumenting about 1 Gt in total and its detection energy threshold is similar to ANTARES. Each detector block contains 115 detection units. A detection unit consists of a string with 18 optical modules. The ORCA detector has one detector block that instruments about 5.7 Mt optimized for atmospheric GeV neutrinos. The total number of strings and OMs in ORCA is the same as in one ARCA block, but the detector elements are placed closer to each other to improve the detector sensitivity at lower energies.

The KM3NeT detectors use new directional optical modules (DOMs) that host 31 3-inch PMTs each. Each DOM has a total PMT photocathode effective area similar to the ANTARES storey with three 10-inch PMTs. Multi-PMT technology allows better light direction estimation and better optical background suppression by using time coincidence between PMT signals. PMTs and their digitization electronics as well as positioning/calibration instrumentation for each DOM are stored inside a 17-inch glass sphere (the same one that is used to store one ANTARES PMT). This concept allows furling of the detection unit for the deployment which makes possible to deploy several detector units during each marine operation. Both detector sites have the underwater infrastructure ready and data taking is started with two detection units at the ARCA site.

For the prompt supernova neutrino detection the method of the optical background suppression using correlated signal between neighbor PMTs was developed for the ANTARES detector. Its

[1] www.asterics2020.eu

natural extension for the KM3NeT multi-PMT DOMs is presented here. The detector response simulation is discussed in Section 3, the benchmark supernova neutrino emission model used is summarized in Section 4 and the analysis optimization is shown in Section 5.

3. Detailed DOM simulation

The detailed simulation is the very first step of the full simulation of ANTARES and KM3NeT [6]. It handles primary particle propagation (positrons, laser light) or radioactive source decay (^{40}K) as well as secondary particles production (Cherenkov photons) and their propagation. The OM technical drawings are reproduced in simulation and photons propagation is done until photoelectron production. This simulation is used to produce the optical module angular acceptance table, which contains the proportion of detected photons for different incidence angles and wavelengths. These tables serve as an input for the full detector simulation. A detailed simulation was chosen for this work because low-energy positrons will be seen mainly by closely located DOMs and the structure of the DOMs may have a non negligible impact on the angular acceptance.

For the detailed simulation standard Geant4[2] libraries are used for particle tracking. The photon tracking is done till the photocathode layer with rather common low-energy Geant4 processes setup. The photocathode layer thickness is of the order of tens of nanometers which is less than the wavelength. The set glass-photocathode-vacuum is a thin-film optical system where coherent wave interference occurs. The light reflection, transmittance and absorption were simulated using analytical calculation with complex wave phases [7]. The light absorption at the photocathode is defined by real refractive indices for glass and vacuum, by the complex refractive index of the photocathode (imaginary part describes the wave attenuation) and by the photocathode thickness. Since the measurements of the photocathode refractive index have big uncertainties, the tuning of the imaginary part was done in order to reproduce the quantum efficiency of the photocathode. The measurements of the quantum efficiency are performed in the lab for a large set of 3-inch PMTs using different wavelengths and illumination of the central part of the PMT with a normally falling beam [8]. The absolute value of the electron escape probability and the signal amplification efficiency (collection efficiency) are tuned using data from the first deployed DOMs [9, 10, 11]. The short-time correlated signal between PMTs coming mainly from ^{40}K decay is used for this purpose similarly to ANTARES [12].

4. Supernova signal simulation

Simulations of the supernova explosions are well advanced nowadays and reproduce the detected spectra and time distributions of the only so far existing SN1987A detection (for a review see, for example, [13]). A variety of models and parameters is present and used by different experiments for sensitivity estimations. Often, there is no overlap between the models used by different experiments, which complicates the direct comparison. In order to overcome this complexity a simplified model is proposed in this work (Section 4.1). In fact, it is very similar to the approach used by the JUNO collaboration ([14]). A new analysis is also introduced later (Section 4.2) using time dependent fluxes computed from latest 3D SN explosion simulations.

[2] geant4.web.cern.ch

In both approaches the SN neutrino spectrum is modeled in terms of the Γ distribution according to the following expression:

$$\frac{d\Phi^{\nu}}{dE_{\nu}}(E_{\nu},t) = \frac{L(t)^{\nu}_{SN}}{4\pi d^2} \times f(E_{\nu},\tilde{E}_{\nu}(t),\alpha(t)), \tag{4.1}$$

$$f(E_{\nu},t) = \frac{E_{\nu}^{\alpha}}{\Gamma(\alpha+1)}(\frac{\alpha+1}{\tilde{E}_{\nu}})^{(\alpha+1)} exp[-\frac{E_{\nu}(\alpha+1)}{\tilde{E}_{\nu}}], \tag{4.2}$$

which is defined with average energy $\tilde{E}_{\nu}$ and spectral shape/pinching parameter α. As it was shown in [15], the neutrino spectra are always fitted with parameters in the range of $2 \lesssim \alpha \lesssim 5$.

4.1 Simplified approach

Results of different supernova simulations predict about $15\% - 25\%$ of the $\bar{\nu}_e$ emission in the first 100 ms. In this approach, a steady flux during this period is assumed. The total ν flux considered by JUNO and generally accepted as a benchmark is 3×10^{53} erg divided equally among the 3 flavors and $\nu/\bar{\nu}$. The more precise fraction of the $\bar{\nu}_e$ flux in the total flux corresponds to $1/5\cos^2\theta_{12} \approx 0.14$, which includes oscillations in supernova mantle [16] and it is close to $1/6$. The shape parameter α is around 3 during this interval, as also chosen by JUNO. The average energy for $\bar{\nu}_e$ is about 15 MeV. In JUNO three values are considered: 12 MeV, 14 MeV and 16 MeV.

The cross-sections for inverse beta decay (IBD) are taken from [16]. The positron energy is calculated as:

$$E^{CM}_{e^+} = \frac{m_p^2 - m_n^2 + m_e + 2E_{\nu}m_p}{2\sqrt{m_p^2 + 2m_pE_{\nu}}} \approx E_{\nu} - \frac{m_n^2 - m_p^2 - m_e^2}{2m_p} \approx E_{\nu} - 1.239\,\text{MeV}, \tag{4.3}$$

where $E_{\nu} \ll m_p$ is considered. As the Lorentz factor of the central mass frame is small for $E_{\nu} \ll m_p$ as well, $E^{CM}_{e^+} \approx E_{e^+}$ (in the lab frame).

The positron distribution as a differential number of particles in 1 kton detector volume from a SN at $D = 10$ kpc was calculated according to the following formula:

$$dN_{e^+}/dE = \frac{1}{F}E_{\nu}^{\alpha}e^{-(\alpha+1)E_{\nu}/\tilde{E}_{\nu}}\{f_{100\text{ ms}}\frac{E^{\text{tot}}_{\bar{\nu}_e}}{\tilde{E}_{\nu}}\}\frac{1}{4\pi D^2}\sigma_{IBD}\{M_{\text{det}}/\mu_{\text{H}_2\text{O}}N_{\text{A}} \times 2\}, \tag{4.4}$$

where $1/F$ is the normalization factor for the neutrino energy distribution from (4.2), $f_{100\text{ ms}} = 25\%$ used, $E^{\text{tot}}_{\bar{\nu}_e} = 3 \times 10^{53}/6$ erg. The first brackets present the calculation of the number of neutrinos at the source.

The previous analysis done for ANTARES [17] used model 57 from [18]. According to this model, there are 65.7 positrons per kiloton of the detector in the first 100 ms and their spectrum follows the distribution described by the following parametrization:

$$dN/dE \sim \frac{E[\text{MeV}]^2}{1 + e^{\frac{E[\text{MeV}]-16}{6}}}. \tag{4.5}$$

The shape of the distribution is similar to the previously described model with $\tilde{E}_{\nu} = 16$ MeV. Also the total numbers of positrons in 1 kton are similar: 45.7, 53.6 and 61.1 for 12 MeV, 14 MeV and 16 MeV correspondingly. The positron generator with both parameterizations of the energy spectrums and isotropic directions was added to the detailed DOM simulation.

4.2 Full MC neutrino interaction generator

Beyond the simplified approach described above, a more detailed simulation of the neutrino interactions was started with the aim of exploring the time and directionality of the supernova neutrino events. A low energy neutrino MC generator was developed including the interactions of $\overline{\nu}_e$ with protons (Inverse Beta Decay, IBD) and the Elastic Scattering (ES) of all neutrino flavors with electrons. These interactions are simulated in a sphere of 10 m radius around a DOM.

This simulation uses fluxes computed from simulations of the Garching group [19] using the expression in (4.2), for a 27$\odot$ progenitor, for a SN occurring at a distance of 10 kpc and for the selected privileged direction (violet direction in [19]). Cross sections are taken from [16] for IBD and [20] for ES. The interaction rates, shown in Figure 1, are computed using the above-mentioned flux and cross-sections. The scattering angle dependent lepton spectrum is now used for getting the

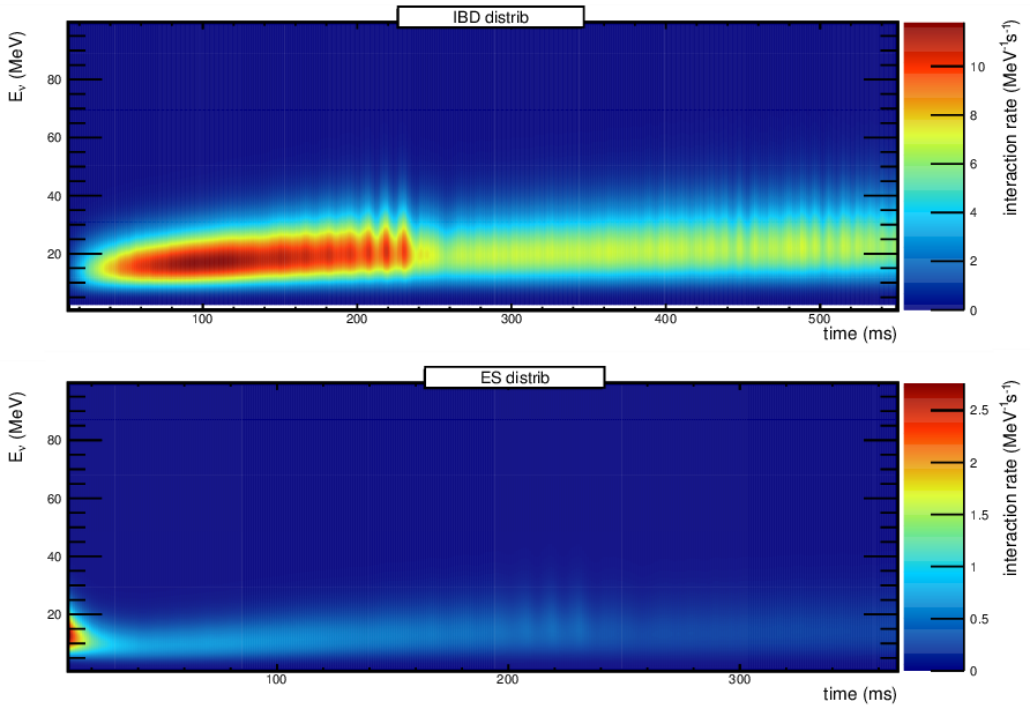

Figure 1: IBD (top) and ES (bottom) interaction rates in the generated volume: 4.2 kton of water.

information of each interaction. The positron energy for IBD is calculated as:

$$E_e = \frac{(E_\nu - \Delta m)(1+\frac{E_\nu}{m_p}) + \frac{E_\nu}{m_p} cos\theta \sqrt{(E_\nu - \Delta m)^2 - \frac{m_e^2}{\kappa}}}{\kappa}, \tag{4.6}$$

where, $\Delta m = m_n^2 - m_p^2 - \frac{m_e^2}{2m_p}$ and $\kappa = (1+\frac{E_\nu}{m_p})^2 - (\frac{E_\nu}{m_p} cos\theta)^2$. The ES electron energy is given by:

$$E_e = \frac{m_e(1+\frac{E_\nu}{m_e})^2 + \frac{E_\nu^2 cos\theta^2}{m_e}}{(1+\frac{E_\nu}{m_e})^2 - (\frac{E_\nu}{m_e} cos\theta)^2}. \tag{4.7}$$

In (4.6-4.7), θ is the scattering angle, i.e. the angle between the incoming ν and the outgoing e^+/e^-. For the selection of the outgoing particles, we use the angular differential cross section to

account for the directionality dependence of their energy. A simplified DOM model is used for this simulation assuming each PMT as a flat disc with the photon detection efficiency calculated with detailed simulation for each incident angle and wavelength. Geant4 is used for the particles tracking and the water properties are simulated according to the latest measurements from ANTARES.

5. Sensitivity optimization

The main optical background in the deep sea water arises from the ^{40}K decay that goes mostly with a 1.3 MeV electron production. Atmospheric muons represent also background for this measurement. Their contribution was taken from the data directly [9, 10]. For simplicity, and based on preliminary measurements, the muon rate for the ARCA site was taken as 1/4 of the muon flux at the ORCA site; lower atmospheric muon rate at ARCA site is due to ∼1 km bigger depth.

To suppress the background, the coincidence method was developed for ANTARES [17]. Instead of all PMT signals, only coincident signals between two or three nearby PMTs (from the same storey) in a short time window (∼20 ns) are used. The sensitivity estimations using these double and triple coincidence selections yield similar results (the sensitivity is about 5 sigma for a SN at 5 kpc). For the KM3NeT detectors, since there are 31 nearby PMTs located in each DOM, higher coincidence level selections can be applied. The rate of hit selections with different coincidence levels in a single DOM is shown in Figure 2 for ^{40}K and muon backgrounds. For the SN signal the steady emission during 100 ms is shown on the same plot for comparison. As it can be seen, the

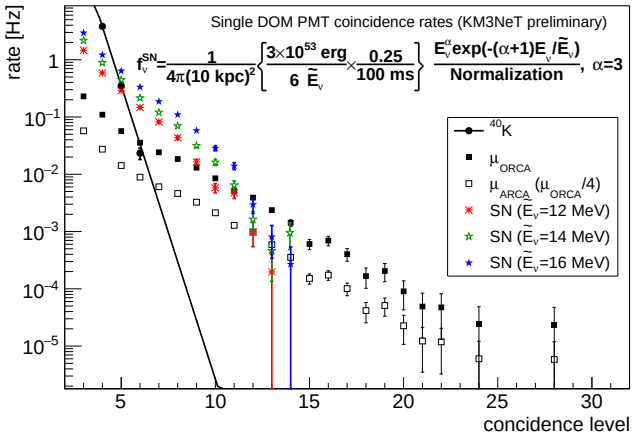

Figure 2: Coincidence event rates for the first 100 ms of the SN explosion (assuming constant emission during this period) for different mean neutrino energies. Main backgrounds (^{40}K decays and atmospheric muons) are also shown.

^{40}K decays produce in general events with fewer coincident hits in a DOM compared to SN events, while atmospheric muons produce a harder coincidence spectrum. This correlates with the lepton energies (1.3 MeV e^- for ^{40}K, $\gtrsim$ 10 MeV e^+ for SN and MeV–GeV energies for μ) and suggests that the coincidence level can be used as a rough event energy estimator.

For known signal and noise rates during a limited period T, the sensitivity can be estimated as:

$$S = \frac{N_{\mathrm{DOMs}} \times T \times f_{\mathrm{SN}}}{\sqrt{N_{\mathrm{DOMs}} \times T \times f_{\mathrm{bg}}}} = \frac{f_{\mathrm{SN}}}{\sqrt{f_{\mathrm{bg}}}} \sqrt{T \times N_{\mathrm{DOMs}}}, \tag{5.1}$$

Table 1: Summary of the results on the SN prompt emission detection with KM3NeT.

$\tilde{E}_{\bar{\nu}_e}$ **MeV**	N_{events} **per block**	$D_{5\sigma/3\sigma}$ **(kpc) ARCA**	$D_{5\sigma/3\sigma}$ **(kpc) ORCA**
12	60	23/30	16/20
14	100	29/37	19/25
16	150	37/47	24/31

where N_{DOMs} is the total number of the DOMs in the detector. Note, that the numerator in the first equation represents expected number of the DOMs detecting supernova signal with a desired coincidence level (expected number of supernova events).

The sensitivity decreases with source-detector distance as $1/D^2$ following the positron production decrease with a distance (4.4). For the $\tilde{E_\nu} = 16$ MeV model one can estimate a 5 sigma sensitivity up to 36 kpc for ARCA (all Milky Way) and 24 kpc for ORCA (95% of the Galactic progenitors). A lower sensitivity of 3 sigma is reached up to 47 kpc for ARCA (the Large Magellanic Cloud is at 50 kpc and its size is ∼4.3 kpc) and up to 31 kpc for ORCA (all Milky Way). The complete set of results is summarized in Table 1. The requirement for an experiment to participate in SNEWS is an average alarm rate of no more than one per week [21], Section 4.3.1. To fulfill this requirement the trigger threshold should be set to 5.1 sigma for 100 ms search frame. These results are rather preliminary; a study of muon veto using coincidences between DOMs can significantly improve the sensitivity.

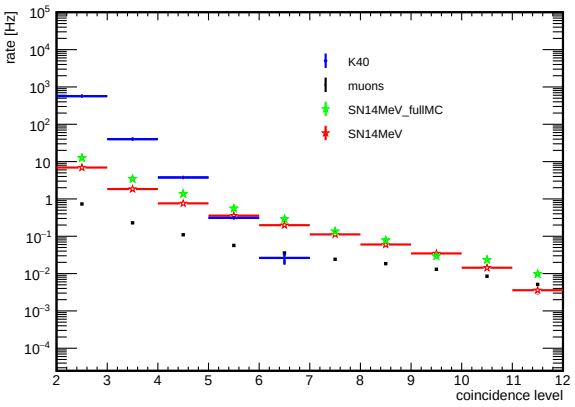

Figure 3: Results of the cross checking between both studies for the case of $\tilde{E}_\nu$=14 MeV.

A preliminary study applying the time dependent flux and taking into account the direction of particles reaches 2.5 sigma sensitivity for a SN at 10 kpc using the model described in Section 4.2 for the ORCA detector. The difference between the two results comes from the fact that the flux model used in the simplified approach predicts a total $\overline{\nu}_e$ luminosity which is larger than the one predicted by the flux model in 4.1 used in the latest 3D SN simulations [19]. However, a crosscheck between both approaches has been done and yields similar results, as one can see in figure 3. The smaller discrepancies can be explained by the different assumptions made in each case, detailed in Sections 4.2 and 4.1. A more detailed study to constrain the SN flux models needs to be done in order to converge in solid results.

6. Conclusion and outlook

Detailed Geant4 simulation of the KM3NeT optical modules is used in this work to estimate the KM3NeT detectors sensitivity to detect prompt emission from supernovae. Both the ARCA and ORCA detectors showed promising sensitivities to Galactic supernovae. Several analysis improvements are expected in the future including ongoing work on muon background suppression.

A generator for low energy supernovae neutrinos has been developed according to the recent 3D supernovae simulations, using a time-dependent flux. This will allow a more sophisticated study of the sensitivity and capability of the detectors to resolve the time variation of the neutrino flux and reconstruct the direction of the source.

References

[1] S. Adrián-Martínez et al, *J. of Phys. G* 43 (2016) 084001

[2] R. Coniglione, *Proceedings of XXV European Cosmic Ray Symposium* (2017) arXiv:1701.05849

[3] S. Adrián-Martínez et al, *JCAP* 02 (2016) 062

[4] A. Albert et al, *MNRAS* 469 (2017) 906

[5] M. Ageron et al, *Nucl. Instrum. Meth. A* 656 (2011) 11

[6] C. Hugon, *PoS ICRC2015* (2016) 1106

[7] D. Motta and S. Schönert, *NIM A* 539 (2005) 217

[8] L. Classen, O. Kalekin, *NIM A* 725 (2013) 155

[9] S. Adrián-Martínez et al, *Eur. Phys. J. C* 74 (2014) 3056

[10] S. Adrián-Martínez et al, *Eur. Phys. J. C* 76 (2016) 54

[11] K. Melis and M. Jongen, this conference

[12] I. Salvadori, this conference

[13] A. Mirizzi et al, *Riv. Nuovo Cimento* 39 (2016) 1

[14] F. An et al, *Phys. G* 43 (2016) 030401

[15] I. Tamborra. et al, *Phys. Rev. D 86* (2012) 125031

[16] A. Strumia and F. Vissani, *Phys. Lett. B* 564 (2003) 42

[17] V. Kulikovskiy 2011, *Proceedings of ICRC 2011* dx.doi.org/10.7529/ICRC2011/V07/1083

[18] A. Burrows, *APJ* 334 (1988) 891

[19] I. Tamborra et al., *ArXiv e-prints 1406.0006* (2014)

[20] G. Radel and R. Beyer, *Mod. Phys. Lett. A*, 08 (1993) 12

[21] P. Antonioli, *New J. Phys.* 6 (2004) 114